

# EFFECT OF ALKYL CHAIN LENGTH OF *o*-HYDROXYOXIME ON THE EXTRACTION OF COPPER

YOSHIKAZU MIYAKE, YASUNOBU IMANISHI, YUJI KATAYAMA,  
TOSHITSUGU HAMATANI AND MASAOKI TERAMOTO

*Department of Industrial Chemistry, Kyoto Institute of Technology, Kyoto 606*

**Key Words:** Extraction, Hydroxyoxime, Interfacial Reaction, Extraction Mechanism, Metal Complex Formation, Diffusion Equation, Interfacial Excess Quantity

The solvent extraction of copper by use of the homologous series of *o*-hydroxyoxime with different alkyl chains was studied to elucidate the extraction mechanism. The physicochemical properties of hydroxyoxime required to evaluate the extraction rate, such as the distribution constant, interfacial properties,  $pK_a$  and extraction constant, were measured. The forward and stripping extraction rates were measured by a Lewis-type transfer cell. The extraction rate of copper by a water-soluble, surface-inactive agent can be reasonably interpreted by considering the diffusion process with complex formation in the aqueous stagnant layer. Complex formation is limited by the rate of 1:1 complex formation. On the other hand, the extraction rate with an insoluble, surface-active reagent can be interpreted by the interfacial reaction, which is limited by the reaction rate between the adsorbed 1:1 complex and the dissolved reagent in the aqueous phase.

## Introduction

Proprietary reagents in current use for the extraction of copper are all of the *o*-hydroxyoxime type, such as LIX series and SME 529. To clarify the mechanism of solvent extraction of metal ion by these commercial chelating agents, it is most important to decide where chelate complex formation occurs. There are two different views on the locus of chelate formation. Freiser *et al.*<sup>1,2)</sup> claimed that the metal complex is produced in the aqueous phase. On the other hand, Flett *et al.*,<sup>4)</sup> Komasaawa *et al.*<sup>8,9)</sup> and Miyake *et al.*<sup>11)</sup> claimed that the reaction of metal complex formation occurs at the organic-aqueous interface because commercial chelating agent has very low solubility in the aqueous phase.

As the commercial *o*-hydroxyoximes are surface-active, the extraction mechanism is more complicated than that by surface-inactive agents, such as benzoylacetone and dithizone. Experimental results showing that the rate-determining step of the interfacial reaction is 1:2 complex formation<sup>4,8,11)</sup> are in conflict with Eigen's mechanism, by which the rate-determining step in the aqueous phase is 1:1 complex formation. The reason for the disagreement has not yet been elucidated.

A useful approach to solving these problems is to study systematically the rates of solvent extraction of metal ions by the homologous series of *o*-hydroxyoxime. However, very few studies have been

made from this point of view.<sup>15,16)</sup> The aim of this paper is to provide a reasonable interpretation for these problems by use of the homologous series of *o*-hydroxyoxime. Some homologs of *anti*-2-hydroxy 5-nonylaceto-phenone oxime, active species of SME 529, were synthesized and used as extractants of copper.

## 1. Experimental

### 1.1 Preparation of organic and aqueous phases

*o*-Hydroxyoximes used as extractants are summarized in **Table 1**. 2-Hydroxy acetophenone oxime (*o*-HAPO), 2-hydroxy 5-methyl acetophenone oxime (HMAPO) and 2-hydroxy-5-ethyl acetophenone oxime (HEAPO) were synthesized.<sup>18)</sup> 2-hydroxy 5-nonyl acetophenone oxime (HNAPO) was purified from SME 529, obtained from Shell Chemical Co. of Japan, Ltd., according to the procedure of Preston and Whewell.<sup>14)</sup> The purity of these oximes was found to be more than 97% by use of H-NMR, IR and mass spectrometer. However, it is unknown whether the nonyl-group of purified HNAPO is normal or branched-chain.

A weighed quantity of the oxime was dissolved in benzene as a stock solution. The concentration of oxime in benzene was determined by a spectrophotometer at 315 nm.

Copper(II) solution was prepared by dissolving copper perchlorate into deionized water. The pH was adjusted to be in the range 2.0–5.0 with perchloric acid or sodium hydroxide, and the ionic strength was adjusted to 0.2 mol/dm<sup>3</sup> with sodium perchlorate. All inorganic chemicals were of analytical grade.

Received September 5, 1985. Correspondence concerning this article should be addressed to Y. Miyake. Y. Imanishi is at Kanzaki Paper Mfg. Co., Ltd., Amagasaki 660. T. Hamatani is at Semi Conductor Energy Laboratory, Atsugi 243.

Table 1. Physicochemical properties of hydroxyoximes

Abbreviation R'	<i>o</i> -HAPO -H	HMAPO -CH <sub>3</sub>	HEAPO -C <sub>2</sub> H <sub>5</sub>	HNAPO -C <sub>9</sub> H <sub>18</sub>
$P_{HR}$ [—]	40	—	130	9100
$pK_a$ [—]	8.7	9.1	9.2	10.4
$\Gamma_{HR}^\infty$ [mol/cm <sup>2</sup> ]	—	—	$3.0 \times 10^{-10}$	$1.8 \times 10^{-10}$
$K_{HR}$ [cm <sup>3</sup> /mol]	—	—	$2.4 \times 10^5$	$2.1 \times 10^6$
$K_{ex}$ [—]	0.2	0.2	0.2	0.2

## 1.2 Measurement of physicochemical properties of oxime

The distribution of oxime between benzene and water phases (volume ratio was 1:5) was obtained according to the usual method.<sup>8)</sup> The concentration of oxime in both phases was measured by a spectrophotometer (Shimadzu UV200S). The activity of oxime in benzene phase was obtained by use of a vapor-pressure osmometry apparatus (Corona 114 type).

The dissociation constant of oxime in the aqueous phase was determined from the change of absorption spectra by pH at constant concentration of oxime, as shown in Fig. 1. The interfacial tension was measured by the pendant drop method.<sup>10)</sup>

When *o*-HAPO was used as the ligand, the kinetics of the chelate formation process in the aqueous phase was studied. However, kinetic information could not be obtained because the 1:1 complex,  $CuR^+$ , is very unstable and the 1:2 complex is poorly soluble in the aqueous phase. Therefore, the rates of 1:2 complex formation were measured in 80 wt% methanol solution by the use of a stopped-flow apparatus (Union Gikken type RA-100). To obtain the exponential transient under the pseudo-first order condition, the copper concentration was adjusted to be much larger than that of *o*-HAPO. The pH in 80 wt% methanol solution was measured by glass/calomel electrode.

## 1.3 Extraction of copper(II)

The distribution of Cu(II) was also obtained by the usual method.<sup>8)</sup> The copper in the organic phase was completely stripped with 6 mol/dm<sup>3</sup> HCl and the concentration of copper in the aqueous phase was analyzed with an atomic absorption spectrophotometer (Nippon Jarrell Ash AA-782).

The transfer cell was the same as used in the previous study.<sup>11,12)</sup> The experimental procedure was similar to that previously mentioned,<sup>11)</sup> except that the agitation speeds of both phases were controlled at 1.75 s<sup>-1</sup>. The initial forward and stripping rates were calculated from the initial slope of time course of copper concentration of organic and aqueous phases, respectively.

All experiments were carried out at 298 K.

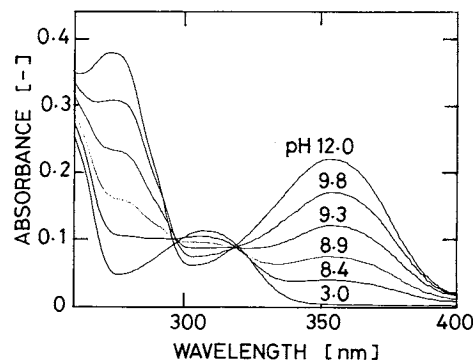
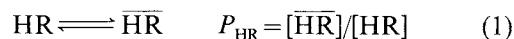


Fig. 1. Changes of absorption spectra of *o*-HAPO by pH in aqueous phase.

## 2. Results and Discussion

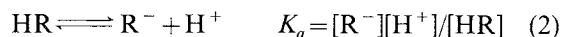
### 2.1 Physicochemical properties of oximes

The experimental results of the distribution constants of oximes (abbreviated HR), defined by Eq. (1), are shown in Table 1.



As expected, this value increases with increasing alkyl chain length. The activity of oxime in benzene was explained in terms of the ideal mixture of monomer and dimer species of oxime. The dimerization constant for HNAPO was obtained as 6 mol/dm<sup>3</sup> at 313 K. Therefore, the dimerization of oxime in benzene can be neglected at the condition,  $C_{HR} < 0.01$  mol/dm<sup>3</sup>.

The proton dissociation of oxime in the aqueous phase is expressed as



As shown in Fig. 1, the absorbance at 355 nm, which is assigned to  $R^-$ , increased with increasing pH. The absorbance in the aqueous phase is expressed by

$$A = \epsilon_R[R^-] + \epsilon_{HR}[HR] \quad (3)$$

The mass balance equation is

$$[HR]_t = [R^-] + [HR] \quad (4)$$

From Eqs. (2) to (4), the following equation can be derived:

$$(A - \epsilon_R[HR]_t)/(\epsilon_{HR}[HR]_t - A) = [H^+]/K_a \quad (5)$$

Since the absorbance of HR can be neglected at 355 nm as shown in Fig. 1, Eq. (5) is simplified to

$$\log(A_e/A - 1) = -pH + pK_a \quad (6)$$

where  $A_e$  is the maximum absorbance at 355 nm.

$$A_e = \epsilon_R[R^-] = \epsilon_R[HR]_t \quad (7)$$

These relations for oximes used are shown in Fig. 2. The values of  $pK_a$  obtained by this method are summarized in Table 1. It is found that the proton of

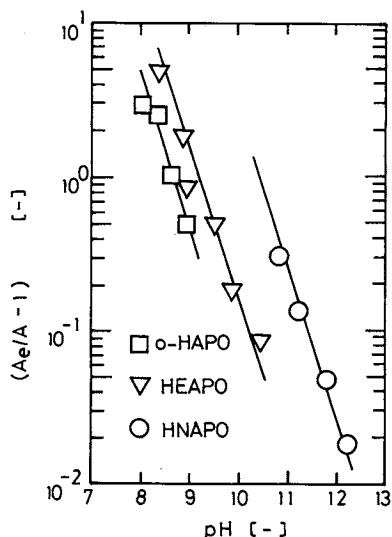


Fig. 2. Relation of Eq. (6) to obtain  $pK_a$  of oxime.

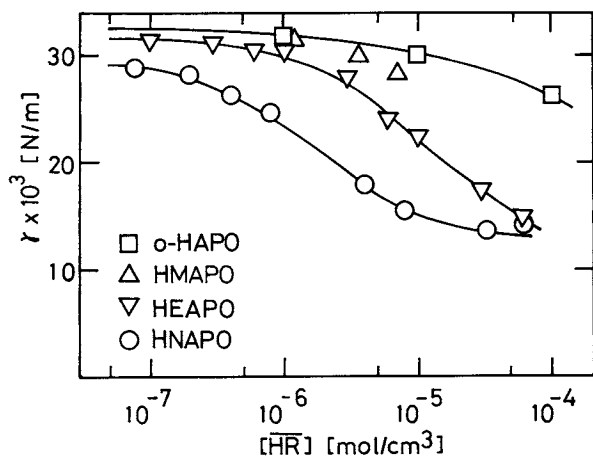


Fig. 3. Interfacial tension between the aqueous and organic phases dissolving oxime.

the hydroxy group at ortho position tends to dissociate in the order (*o*-HAPO) > (HMAPO) > (HEAPO) > (HNAPO).

The plots of the interfacial tension against the total concentration of oxime in benzene are shown in Fig. 3. The interfacial tension lowering for *o*-HAPO was negligibly small up to about  $1.0 \times 10^{-5}$  mol/cm<sup>3</sup>. The interfacial excess quantity calculated by the Gibbs equation can be correlated by the Langmuir adsorption isotherm,<sup>11)</sup> Eq. (8).

$$\Gamma_{HR}/\Gamma_{HR}^{\infty} = (1 + 1/(K_{HR}[\overline{HR}]))^{-1} \quad (8)$$

The constants  $\Gamma_{HR}^{\infty}$  and  $K_{HR}$  are shown in Table 1. The value of  $\Gamma_{HR}^{\infty}$  is almost constant, but  $K_{HR}$  increased with increasing chain length of the alkyl group. This means that interfacial activity increases with increasing chain length of the alkyl group. It was also found that the presence of the copper complex of HNAPO does not affect the interfacial tension.<sup>19)</sup>

## 2.2 Copper(II) extraction equilibrium

The distribution ratio of Cu(II),  $D_{Cu} = [\overline{CuR_2}]/$

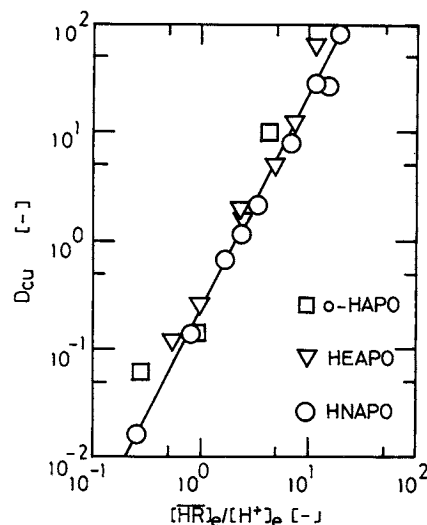


Fig. 4. Relation between the distribution ratio of copper and the concentration ratio  $[HR]/[H^+]$ .

$[Cu^{2+}]$ , is plotted against the concentration ratio,  $([HR]/[H^+])_e$ , in Fig. 4. The observed data fall on a single line with a slope of 2.0 irrespective of kind of oxime. The overall reaction for Cu(II) extraction with oxime is expressed as



$$K_{ex} = [\overline{CuR_2}][H^+]^2 / ([Cu^{2+}][\overline{HR}]^2) \quad (10)$$

The value of  $K_{ex}$  was 0.2 for the oximes used in the present work.

## 2.3 Extraction rate of Cu(II) by *o*-HAPO

(1) Reaction scheme in the aqueous phase *o*-Hydroxyoxime is a weak acidic chelating agent, and the scheme of complex formation with Cu(II) is expressed in Fig. 5. Since the concentration of  $R^-$  is negligibly small under the condition of  $pH \ll pK_a$ , and the 1:1 complex,  $CuR^+$ , is very unstable, a stationary state method can be applied to these species. Then the rate of 1:2 complex formation can be expressed by Eq. (11).

$$r_f = d[CuR_2]/dt \quad (11a)$$

$$= k_{app}([Cu][HR] - [CuR_2][H]^2/K_1K_3[HR]) \quad (11b)$$

$$k_{app}$$

$$= \frac{k_1 + k_2/([H]/K_a + k_2[Cu]/k_a)}{1 + [H]/k_3K_1[HR](k_1 + k_2/([H]/K_a + k_2[Cu]/k_a))} \quad (11c)$$

If the rate of  $CuR_2$  formation (path IV) is very fast, the rate is determined by steps II and III, and the rate constant was simplified as follows.

$$k_{app} = k_1 + k_2/([H]/K_a + k_2[Cu]/k_a) \quad (12)$$

The rate constant in the aqueous solution could not be measured, but the rate constants could be obtained in 80 wt% methanol solution. The relaxation times

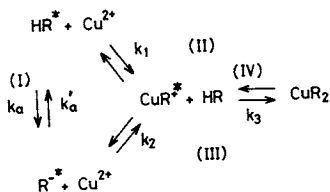


Fig. 5. Scheme of reaction between Cu(II) and oxime in aqueous phase and at the interface. \* denotes adsorptive species.

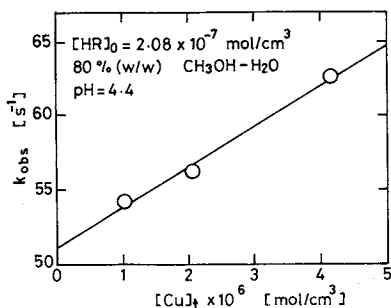


Fig. 6. Relation between pseudo-first order rate constant and cupric concentration in 80 wt% methanol solution.

were calculated from the exponential transient curves for 1:2 complex formation, observed under the condition of  $[\text{Cu}^{2+}] \gg [\text{HR}]$ . The effect of cupric ion concentration on  $k_{\text{obs}}$  ( $=k_{\text{app}}[\text{Cu}]_t$ ) is shown in Fig. 6. Since  $k_{\text{obs}}$  ( $=\tau^{-1}$ ) is proportional to  $[\text{Cu}]_t$ , the term  $[\text{H}^+]/K_a$  in the denominator of Eq. (12) is negligibly small compared to  $k_2[\text{Cu}]/k_a$  in the 80 wt% methanol solution. Then, the values of  $k_1$  and  $k_a$  were calculated from the slope and the intercept of the straight line as  $2.5 \times 10^6 \text{ cm}^3/(\text{mol} \cdot \text{s})$  and  $52 \text{ s}^{-1}$ , respectively.

The value of  $k_1$  is much lower than that estimated from Eigen's mechanism,  $8 \times 10^{10} \text{ cm}^3/(\text{mol} \cdot \text{s})$ . This feature is also observed in the reaction between benzoylacetone and Cu(II).<sup>6)</sup> The rate-determining step of step II is not the release of coordinated water from cupric ion, but is the proton release from the transient intermediate Cu-HR.

The rate of the proton association with  $\text{R}^-$  is very fast, and is limited by the diffusion of  $\text{H}^+$  and  $\text{R}^-$ . Then, the value of  $k_a'$  can be estimated by the diffusion-controlled rate expression of Debye.<sup>3)</sup>  $k_a$  can be obtained from the relation,  $k_a = K_a k_a'$ , as  $70 \text{ s}^{-1}$  for *o*-HAPO in aqueous phase. The observed  $k_a$  in 80 wt% methanol solution is close to this value.  $k_1$  in the aqueous phase cannot be estimated by Eigen's mechanism and was taken as an adjustable parameter. The value of  $k_a$  in aqueous phase can be estimated from the observed  $K_a$  and the estimated  $k_a'$  by Debye's theoretical equation. If it is assumed that the reaction between the dissociated hydroxyoxime and Cu(II) follows Eigen's mechanism, the value of  $k_2$  can be estimated as  $5.0 \times 10^{11} \text{ cm}^3/(\text{mol} \cdot \text{s})$ .<sup>17)</sup>

(2) Forward extraction rate It is deduced that the chelation of Cu(II) with *o*-HAPO mainly proceeds in

the aqueous phase because *o*-HAPO is water-soluble and surface-inactive. The diffusion equations in the aqueous stagnant layer are given by

$$D d^2[\text{HR}]/dx^2 = 2r_f, \quad D d^2[\text{CuR}_2]/dx^2 = -r_f \quad (13a)$$

with the boundary condition:

at  $x=0$  (interface)

$$[\text{HR}] = [\text{HR}]_i, \quad [\text{CuR}_2] = [\text{CuR}_2]_i \quad (13b)$$

$$J_{\text{HR}}^a = -D d[\text{HR}]/dx, \quad J_{\text{CuR}_2}^a = -D d[\text{CuR}_2]/dx \quad (13c)$$

at  $x=x_L$  (the edge of aqueous stagnant layer)

$$[\text{HR}] = [\text{CuR}_2] = 0 \quad (13d)$$

Here, the diffusion coefficient is assumed to be constant irrespective of diffusing species, for the sake of simplicity. To obtain the approximate solution of these ordinary differential equations, Eq. (11) is linearized as

$$r_f = k_f[\text{HR}] - k_r[\text{CuR}_2] \quad (14a)$$

$$k_f = k_{\text{app}}[\text{Cu}]_i, \quad k_r = k_{\text{app}}[\text{H}]_i^2/(K_1 K_3 [\text{HR}]_i) \quad (14b)$$

Then Eq. (13) can be solved and the flux of  $\text{CuR}_2$  from interface to aqueous bulk is expressed as

$$J_{\text{CuR}_2}^a = k_w[\text{CuR}_2]_i - (k_f^b[\text{HR}]_i - k_r^b[\text{CuR}_2]_i) \quad (15a)$$

$$k_f^b = k_w(\beta - 1)K/(1 + K)/2 \quad (15b)$$

$$K = 2k_f^b/k_r^b = 2K_1 K_3 [\text{HR}]_i [\text{Cu}]_i / [\text{H}]_i^2 \quad (15c)$$

$$\beta = \gamma_a \coth \gamma_a \quad (15d)$$

$$\gamma_a = (2k_f(1 + K^{-1})D)^{0.5}/k_w \quad (15e)$$

The mass balance equation of  $\text{CuR}_2$  at the interface is expressed as

$$k_o^c[\overline{\text{CuR}_2}]_i + J_{\text{CuR}_2}^a = \delta r_f^* \quad (16a)$$

$$\delta r_f^* = k_f^*[\overline{\text{HR}}]_i - k_r^*[\overline{\text{CuR}_2}]_i \quad (16b)$$

$$k_f^* = \delta k_{\text{app}}[\text{Cu}]_i \quad (16c)$$

$$k_r^* = 2k_f^*(P_{\text{HR}}/P_{\text{CuR}_2})/K \quad (16d)$$

The right-hand side of Eq. (16a) is the formation rate of  $\text{CuR}_2$  in the interfacial zone per unit area, and  $\delta$  is the thickness of the interfacial zone. The forward extraction rate is calculated by

$$J_f = k_o^c[\overline{\text{CuR}_2}]_i \quad (17a)$$

$$= \frac{(k_f^b/P_{\text{HR}} + k_f^*)[\text{HR}]_i}{1 + k_w/(k_o^c P_{\text{HR}}) + 2(P_{\text{HR}}/P_{\text{CuR}_2})(k_f^b/P_{\text{HR}} + k_f^*)/k_o^c K} \quad (17b)$$

The first and second terms in the numerator of Eq. (17b) are the formation rate of  $\text{CuR}_2$  in the aqueous stagnant layer and that in the interfacial zone, respectively. The second and third terms in the de-

nominator of Eq. (17b) are the loss of  $\text{CuR}_2$  to the aqueous phase and the contribution of reverse reaction rate, respectively. The interfacial concentration of each species can be calculated from the mass balance equations at the interface.

$$k_w^m([\overline{\text{HR}}]_b - [\overline{\text{HR}}]_i) = k_w([\text{HR}]_i + 2[\text{CuR}_2]_i) + 2k_o^c[\overline{\text{CuR}_2}]_i \quad (18a)$$

$$g = 1 + 2K_d(k_o^d/k_o^m)([\overline{\text{HR}}]_b + [\overline{\text{HR}}]_i) \quad (18b)$$

$$k_w[\text{CuR}_2]_i + k_o^c[\overline{\text{CuR}_2}]_i = k_w([\text{Cu}]_b - [\text{Cu}]_i) \quad (18c)$$

$$k_w[\text{CuR}_2]_i + k_o^c[\overline{\text{CuR}_2}]_i = k_w([\text{H}]_i - [\text{H}]_b)/2 \quad (18d)$$

The coefficient  $g$ , which is expressed by Eq. (18b) was introduced to take into account the diffusion of both monomer and dimer of the free extractant.

**Figures 7(a), (b) and (c)** show the effects of  $[\text{H}]$ ,  $[\text{Cu}]$  and  $[\text{HR}]$  on the forward extraction rate, respectively. The solid lines in Fig. 7 were calculated from Eq. (17) and Eq. (12) by use of the observed and estimated values of parameters shown in **Table 2**.  $k_1$  and  $\delta$  are adjustable parameters and were given as  $1 \times 10^6 \text{ cm}^3/(\text{mol} \cdot \text{s})$  and  $1 \times 10^{-7} \text{ cm}$ , respectively. This  $k_1$  value is close to the observed one in 80 wt% methanol solution. The value of  $k_f^*$  was negligibly small compared to  $k_f^*/P_{\text{HR}}$ . Thus, the effects of  $[\text{H}]$ ,  $[\text{Cu}]$  and  $[\text{HR}]$  on  $J_f$  can be interpreted satisfactorily by the present model.

**(3) Stripping rate** The reactions in the stripping process occur in the reverse of the path of reactions shown in Fig. 5. Then, the rate of  $\text{Cu(II)}$  formation is related to Eq. (11) as follows.

$$r_r = d[\text{Cu}]/dt = -r_f \quad (19)$$

Since the partition constant of 1:2 complex is as low as 100, it is deduced that the reactions occur in the aqueous stagnant layer. Then the same diffusion equations, Eq. (13), are applied to analyse the stripping rate, and the flux of  $\text{CuR}_2$  can be expressed by Eq. (15).

The mass balance equation for  $\text{CuR}_2$  at the interface are expressed as

$$J_r = k_o^c([\overline{\text{CuR}_2}]_b - [\overline{\text{CuR}_2}]_i) = J_{\text{CuR}_2}^a - \delta r_f^* \quad (20)$$

where  $J_{\text{CuR}_2}^a$  and  $\delta r_f^*$  are expressed by Eqs. (15) and (16), respectively. The mass balance equations for other species at the interface are necessary for estimating the interfacial concentrations and are given as

$$2k_o^c([\overline{\text{CuR}_2}]_b - [\overline{\text{CuR}_2}]_i) = k_w^m([\overline{\text{HR}}]_i - [\overline{\text{HR}}]_b) + k_w([\text{HR}]_i + 2[\text{CuR}_2]_i) \quad (21a)$$

$$k_o^c([\overline{\text{CuR}_2}]_b - [\overline{\text{CuR}_2}]_i) = k_w([\text{Cu}]_i + [\text{CuR}_2]_i) \quad (21b)$$

$$k_o^c([\overline{\text{CuR}_2}]_b - [\overline{\text{CuR}_2}]_i) = k_w([\text{H}]_i - [\text{H}]_b)/2 \quad (21c)$$

**Figures 8(a), (b) and (c)** show the effects of proton

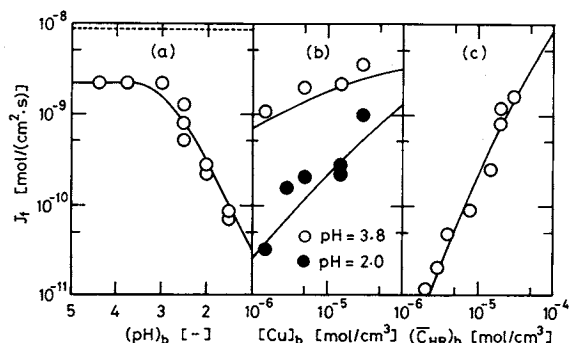


**Fig. 7.** Effects of pH, concentration of  $\text{Cu(II)}$  and concentration of  $o\text{-HAPO}$  on the forward extraction rate of  $\text{Cu(II)}$ .

(a)  $[\text{Cu}]_b = 1.5 \times 10^{-5} \text{ mol/cm}^3$ ,  $[\overline{\text{HR}}]_b = 7.9 \times 10^{-6} \text{ mol/cm}^3$ ; (b)  $[\overline{\text{HR}}]_b = 7.9 \times 10^{-6} \text{ mol/cm}^3$ ; (c)  $[\text{Cu}]_b = 1.5 \times 10^{-5} \text{ mol/cm}^3$ ,  $\text{pH} = 1.5$ .

**Table 2.** Parameters for calculation of extraction rate of cupric ion

	<i>o</i> -HAPO	HNAPO
$k_w^*$ [cm/s]	$1.0 \times 10^{-3}$	$0.8 \times 10^{-3}$
$k_o^{c*}$ [cm/s]	$1.6 \times 10^{-3}$	$7.5 \times 10^{-4}$
$k_o^{m**}$ [cm/s]	$2.1 \times 10^{-3}$	$9.9 \times 10^{-4}$
$k_a^{**}$ [1/s]	70	1.4
$k_1$ [cm <sup>3</sup> /(mol s)]	$1.0 \times 10^6$	$1.0 \times 10^6$
$k_2^{**}$ [cm <sup>3</sup> /(mol s)]	$5.0 \times 10^{11}$	$5.0 \times 10^{11}$
$k_3 K_1$ [cm <sup>3</sup> /(mol s)]	$2.0 \times 10^7$	$8.0 \times 10^7$
$D^{**}$ [cm <sup>2</sup> /s]	$7.7 \times 10^{-6}$	$4.8 \times 10^{-6}$
$\delta$ [cm]	$1.0 \times 10^{-7}$	$1.0 \times 10^{-7}$

\* Observed value. \*\* Estimated value.

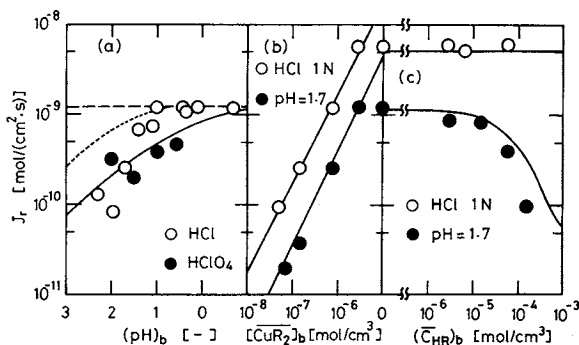


**Fig. 8.** Effects of pH, concentrations of 1:2 complex and free  $o\text{-HAPO}$  on the stripping rate.

(a)  $[\text{CuR}_2]_b = 7.5 \times 10^{-7} \text{ mol/cm}^3$ ,  $[\overline{\text{HR}}]_b = 0.0$ ; (b)  $[\overline{\text{HR}}]_b = 0.0$ ; (c)  $[\text{CuR}_2]_b = 3.0 \times 10^{-6} \text{ mol/cm}^3$ .

activity in the stripping solution and the concentration of 1:2 complex and the concentration of free hydroxyoxime in the organic phase on the stripping rate, respectively. Though the observed data in Fig. 8(a) scatter, no systematic difference is observed for stripping agents. The proton activity at high  $\text{HCl}$  concentration was estimated by use of activity coefficients.<sup>12)</sup> As shown in Fig. 8(c), the stripping rate at  $\text{pH} = 1.7$  decreased with increasing free hydroxyoxime

concentration in the organic phase due to 1:2 complex formation.

The stripping rate limited by the diffusion of 1:2 complex in the organic stagnant layer is shown by the broken line in Fig. 8. The mass transfer coefficient of 1:2 complex,  $k_o^c$ , was evaluated as  $1.6 \times 10^{-3}$  cm/s from this region.

As the proton activity is much higher in the stripping process, the second term in the denominator of Eq. (11c) cannot be neglected in comparison with unity. If the value of  $k_{app}$  is estimated by Eq. (12), the calculated values are higher than the observed ones as shown by the dotted line in Fig. 8(a). Therefore,  $k_{app}$  is evaluated by Eq. (11c). The solid lines are calculated by Eqs. (20) and (21) with the same values of the parameters in evaluating the forward extraction rate and with  $k_3 K_1 = 2 \times 10^7$  cm<sup>3</sup>/(mol·s). The observed data can be interpreted by this model.

## 2.4 Extraction rate of Cu(II) by HNAPO

(1) Reaction scheme at the organic-aqueous interface As HNAPO is less soluble in the aqueous phase and is surface-active, chelate formation may take place at the interface. It is assumed that the reaction mechanism at the interface is similar to that in the aqueous phase as shown in Fig. 5, except that the species HR, R<sup>-</sup> and CuR<sup>+</sup> are surface-active. It is noted that the CuR<sup>+</sup> adsorbed at the interface reacts with HR dissolved in the aqueous phase.<sup>7)</sup> Then, the rate of CuR<sub>2</sub> formation per unit area of the interface is expressed as follows.<sup>7)</sup>

$$\delta r_f^* = k_f^* ([Cu][\overline{HR}] - [H]^2 [\overline{CuR_2}] / k_{ex} [\overline{HR}]) \quad (22a)$$

$$k_f^* = \frac{\left( k_1 + \frac{k_2}{[H] K_{HR} / K_a K_R + k_2 [Cu] / k_a} \right) \{ I_{HR}^\infty K_{HR} / (1 + K_{HR} [\overline{HR}]) + \delta \}}{1 + \frac{[H] K_{HR}}{k_3 K_1 [\overline{HR}] K_{CuR}} \left( k_1 + \frac{k_2}{[H] K_{HR} / K_a K_R + k_2 [Cu] / k_a} \right)} \quad (22b)$$

adsorbed 1:1 complex and HNAPO dissolved in aqueous phase. Thus, the formation rate of CuR<sub>2</sub> at the interface is simplified to

$$\delta r_f^* = (k_3 K_1 / P_{HR}) \{ I_{HR}^\infty K_{HR} / (1 + K_{HR} [\overline{HR}]) + \delta \} \times ([Cu][\overline{HR}]^2 / [H] - [\overline{CuR_2}][H] / K_{ex}) \quad (23)$$

This relation is similar to that derived in the previous paper,<sup>11)</sup> except for the term  $P_{HR}$  in the rate parameter.

(2) Forward extraction rate The effects of pH and the concentrations of cupric ion and HNAPO on the forward extraction rate are shown in Figs. 9(a), (b) and (c), respectively. The dotted line in Fig. 9(a) is the value calculated with  $k_f^* = 0$  in Eq. (17). As the observed value is much higher than the dotted line, the contribution of the formation of CuR<sub>2</sub> in the aqueous stagnant layer to the forward extraction rate

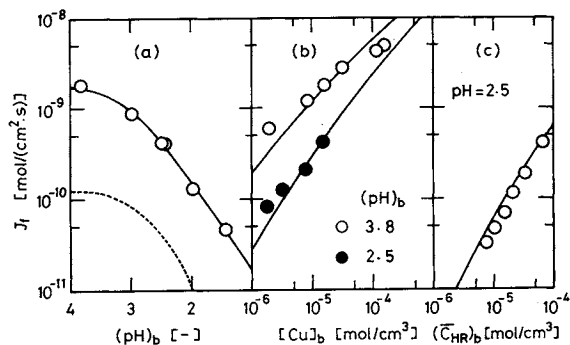


Fig. 9. Effects of pH, concentration of Cu(II) and concentration of HNAPO on the forward extraction rate of Cu(II).

(a)  $[Cu]_b = 1.5 \times 10^{-5}$  mol/cm<sup>3</sup>,  $[\overline{HR}]_b = 6.3 \times 10^{-5}$  mol/cm<sup>3</sup>; (b)  $[\overline{HR}]_b = 6.3 \times 10^{-5}$  mol/cm<sup>3</sup>; (c)  $[Cu]_b = 1.5 \times 10^{-5}$  mol/cm<sup>3</sup>.

If the Langmuir adsorption constants for adsorptive species agree with each other, i.e.,  $K_{HR} = K_R = K_{CuR}$ ,  $k_f^*$  can be simplified as

$$k_f^* = k_{app} \{ I_{HR}^\infty K_{HR} / (1 + K_{HR} [\overline{HR}]) + \delta \} \quad (22c)$$

where  $k_{app}$  is expressed by Eq. (11c). Since the distribution constant of HNAPO is much larger,  $P_{HR} = 9100$ , the concentration of HNAPO in the aqueous phase is much lower. Therefore, the second term in the denominator of Eq. (11c) is greater than unity. This means that the formation rate of CuR<sub>2</sub> at the interface is determined by the reaction between the

is negligibly small. The formation of CuR<sub>2</sub> at the interface dominates the extraction rate.

Then, the forward extraction rate with HNAPO can be estimated by Eq. (17) with the value of  $k_f^*$  by Eq. (22b). The solid lines in Fig. 9 were calculated by use of the parameters expressed in Table 2. The value of the adjustable parameter,  $k_3 K_1$ , was determined so as to fit the experimental data as  $8 \times 10^7$  cm<sup>3</sup>/(mol·s). As the rate constant  $k_f$  used in the previous paper<sup>11)</sup> is equal to  $k_3 K_1 / P_{HR}$  in the present model, the value of  $k_3 K_1$  is calculated as  $1.4 \times 10^8$  cm<sup>3</sup>/(mol·s). This value is approximately equal to the value obtained in this study.

The forward extraction rate of copper with HNAPO could be explained by considering the interfacial reaction mechanism as shown in Fig. 5. As HNAPO is poorly soluble in the aqueous phase, the reaction rate was determined by the reaction between

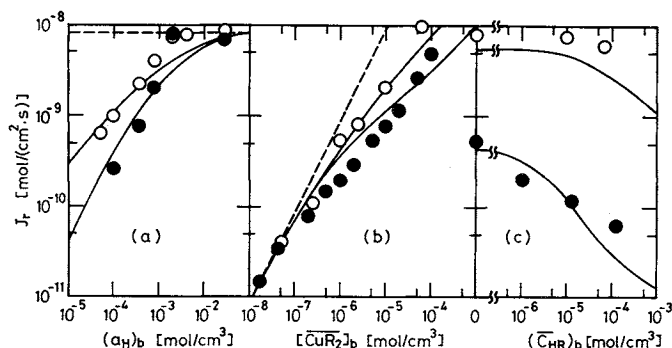


**Fig. 10.** Effects of proton activity and concentration of 1:2 complex and free HNAPO on the stripping rate.

(a)  $[\text{CuR}_2]_b = 10^{-5} \text{ mol/cm}^3$ ,  $[\text{HR}]_b = 0$  ( $\circ$ ),  $10^{-5} \text{ mol/cm}^3$  ( $\bullet$ ); (b)  $[\text{HCl}] = 0.5 \text{ N}$ ,  $[\text{HR}]_b = 0$  ( $\circ$ ),  $[\text{HR}]_b = [\text{CuR}_2]_b$  ( $\bullet$ ); (c)  $[\text{CuR}_2]_b = 10^{-5} \text{ mol/cm}^3$ ,  $[\text{HCl}] = 3 \text{ N}$  ( $\circ$ ),  $[\text{CuR}_2]_b = 10^{-6} \text{ mol/cm}^3$ ,  $[\text{HCl}] = 0.5 \text{ N}$  ( $\bullet$ ).

the adsorbed 1:1 complex and the HNAPO dissolved in aqueous phase.

**(3) Stripping rate** Figure 10(a), (b) and (c) show the effects of the proton activity and the concentration of 1:2 complex and free HNAPO on the stripping rate, respectively. As shown in Fig. 10(a), the observed stripping rate rises asymptotically to a maximum value with increasing proton activity. The presence of this region (broken line in Fig. 10) means that the stripping rate is limited by the diffusion rate of 1:2 complex in the organic stagnant layer and the mass transfer coefficient was calculated as  $7.5 \times 10^{-4} \text{ cm/s}$ . In the lower  $(a_{\text{H}})_b$  range, the stripping rate increases with increasing  $(a_{\text{H}})_b$  and decreases by the addition of free HNAPO in the organic phase.

The  $[\text{CuR}_2]_b$  dependences of the stripping rate are complicated, as shown in Fig. 10(b). The open and black circles show the observed stripping rate for the condition without free HNAPO and for the condition where the concentration of free HNAPO in the bulk organic phase is equal to  $[\text{CuR}_2]_b$ , i.e., the concentration ratio  $[\text{CuR}_2]_b/[\text{HR}]_b = 1.0$ , respectively. At low  $[\text{CuR}_2]_b$ , the stripping rate is proportional to  $[\text{CuR}_2]_b$  and the observed data fall on the broken straight line corresponding to the diffusion limitation of 1:2 complex in the organic stagnant layer. The stripping rate slowly decreases from the broken line with increasing  $[\text{CuR}_2]_b$ . The decrease in stripping rate in the presence of free HNAPO is greater than that without free HNAPO. When HNAPO was added to the organic phase, the stripping rate was again proportional to  $[\text{CuR}_2]_b$  under the condition of  $[\text{CuR}_2]_b = [\text{HR}]_b > 10^{-5} \text{ mol/cm}^3$ . Figure 10(c) shows that the effect of addition of free HNAPO at  $[\text{HCl}] = 0.5 \text{ N}$  is greater than that at  $[\text{HCl}] = 3 \text{ N}$ .

The solid lines in Figs. 10(a), (b) and (c) show the results calculated from Eqs. (20), (21) and (22) by the use of parameters in Table 2. The tendency of the concentration dependences for the stripping rate could be approximately expressed by this model.

As mentioned in the previous paper,<sup>12)</sup> the existence of free HNAPO increases the resistance of the interfacial reaction, because the adsorption of the free HNAPO at the interface decreases the effective interfacial area. This effect is expressed by the term,  $(\Gamma_{\text{HR}}^\infty K_{\text{HR}} / (1 + K_{\text{HR}}[\text{HR}]_i) + \delta)$  in Eq. (22). That is, when the concentration of free HNAPO at the interface is greater than  $K_{\text{HR}} = 5 \times 10^{-7} \text{ mol/cm}^3$ , the stripping rates decrease by this effect. When  $\delta$  is greater than that of  $\Gamma_{\text{HR}}^\infty K_{\text{HR}} / (1 + K_{\text{HR}}[\text{HR}]_i)$ , the stripping rate is independent of the concentration of free HNAPO. The critical concentration of HNAPO was calculated as  $10^{-3} \text{ mol/cm}^3$  by this model. This value is different from the observed value (about  $10^{-5} \text{ mol/cm}^3$ ). One of the reasons for this discrepancy may be that the Langmuir adsorption equation cannot be applied to the adsorption of free HNAPO at the higher concentration or that the value of  $\delta$  is uncertain. Further study of the shielding effect due to the adsorption of surfactant from a more quantitative viewpoint is required.<sup>13)</sup>

## 2.5 Forward extraction rate of Cu(II) at high pH

As shown in Figs. 7(a) and 9(a), the forward extraction rate rises asymptotically to a maximum value with increasing pH. The overall mass transfer coefficient,  $K_o$ , was calculated by Eq. (24).

$$(J_f)_{\text{max}} = K_o [\text{HR}]_b / 2 \quad (24)$$

The calculated values of  $K_o$  were  $5.6 \times 10^{-4} \text{ cm/s}$  for *o*-HAPO,  $1.9 \times 10^{-4} \text{ cm/s}$  for HEAPO and  $8.9 \times 10^{-5} \text{ cm/s}$  for HNAPO, and decreased with the length of the alkyl group. The mass transfer coefficient of *o*-hydroxyoxime,  $k_o^m$ , can be estimated from the value of  $k_o^c$  obtained from the stripping rate, assuming that the mass transfer coefficient is proportional to  $D^{2/3}$  and the molar volume of the 1:2 complex is twice that of the monomer. By use of the Wilke and Chang equation,  $k_o^m$  was obtained as  $2^{0.4} k_o^c$ . The obtained values of  $k_o^m$  are shown in Table 2. These values are greater than those of  $K_o$ , suggesting that other resistance is

involved in  $K_o$ . This resistance  $R_I$  was calculated by Eq. (25).

$$R_I = 1/K_o - 1/k_o^m \quad (25)$$

The results were 1,300 s/cm for *o*-HAPO, 4,600 s/cm for HEAPO and 10,000 s/cm for HNAPO. As steps (I) and (II) of the reaction shown in Fig. 5 are independent of pH, the resistance of this reaction cannot be neglected at higher pH. It was noted that the second term in the denominator of Eq. (22b) is comparable to unity at higher pH; that is, the resistance of the 1 : 1 complex formation increases even in the case of HNAPO. Since the rate of 1 : 1 complex formation was limited by steps (I) and (II) at higher pH, the value of  $R_I$  increases with decreasing value of  $k_a$ , i.e., the value of  $K_a$ . This resistance can be reasonably expressed by the proposed model.

## Conclusions

The solvent extraction of copper by use of the homologous hydroxyoximes with different alkyl chains (*o*-HAPO, HMAPO, HEAPO and HNAPO) was studied to elucidate the extraction mechanism. The physicochemical properties of these hydroxyoximes such as the distribution constant and the interfacial tension between the benzene and aqueous phases and the  $pK_a$  of hydroxyoxime were measured. The extraction constant of copper was obtained as 0.2 for all oximes used.

The extraction and stripping rates were measured by a Lewis-type stirred transfer cell with a constant interfacial area. It was found for the Cu(II)-*o*-HAPO system that the extraction and stripping rates could be interpreted satisfactorily by considering complex formation in the aqueous stagnant layer because *o*-HAPO is water-soluble and surface-inactive. It was also found that complex formation is limited by 1 : 1 complex formation. On the other hand, in the case of copper extraction with HNAPO, which is less soluble and is surface-active, complex formation at the interface is very important and the rate was evaluated by considering the adsorption of reagents. Complex formation at the interface is limited by 1 : 2 complex formation between the adsorbed 1 : 1 complex and the dissolved reagent in the aqueous phase, because of the lower solubility of HNAPO in the aqueous phase.

## Acknowledgment

This work supported in part by a Grant-in-Aid for Scientific Research (No. 60750885) from the Ministry of Education, Science and Culture of Japan. We thank Professor M. Harada, Institute of Atomic Energy of Kyoto University, for useful discussions and for the use of stopped-flow apparatus in their laboratories.

(Presented at Symposium on Solvent Extraction 1983 at Hamamatsu, December 9–10, 1983.)

## Nomenclature

$A$	= absorbance	[—]
$A_e$	= maximum absorbance defined by Eq. (7)	[—]
$C_{HR}$	= concentration of hydroxyoxime in organic phase	[mol/cm <sup>3</sup> ]
$D_{Cu}$	= distribution ratio of copper	[—]
$D$	= diffusivity	[cm <sup>2</sup> /s]
$J_J$	= flux of species $J$	[mol/(cm <sup>2</sup> s)]
$J_f$	= initial forward extraction rate	[mol/(cm <sup>2</sup> s)]
$J_r$	= initial stripping rate	[mol/(cm <sup>2</sup> s)]
$K$	= equilibrium constant defined by Eq. (15c)	[—]
$K_a$	= dissociation constant of hydroxyoxime	[mol/cm <sup>3</sup> ]
$K_d$	= dimerization constant of <i>o</i> -hydroxyoxime in organic	[cm <sup>3</sup> /mol]
$K_{ex}$	= extraction constant of copper	[—]
$K_J$	= Langmuir adsorption constant of species $J$	[cm <sup>3</sup> /mol]
$K_o$	= overall mass transfer coefficient	[cm/s]
$K_1$	= equilibrium constant of reaction step (II)	[—]
$K_3$	= equilibrium constant of reaction step (IV)	[—]
$k_1$	= rate constant of reaction step (II)	[cm <sup>3</sup> /(mol s)]
$k_2$	= rate constant of reaction step (III)	[cm <sup>3</sup> /(mol s)]
$k_3$	= rate constant of reaction step (IV)	[cm <sup>3</sup> /(mol s)]
$k_a$	= proton dissociation rate constant of hydroxyoxime	[s <sup>-1</sup> ]
$k'_a$	= proton association rate constant of hydroxyoxime	[cm <sup>3</sup> /(mol s)]
$k_{app}$	= overall rate constant of formation of CuR <sub>2</sub>	[cm <sup>3</sup> /(mol s)]
$k_o$	= mass transfer coefficient in organic stagnant layer	[cm/s]
$k_{obs}$	= rate constant observed by stopped-flow apparatus	[s <sup>-1</sup> ]
$k_w$	= mass transfer coefficient in aqueous stagnant layer	[cm/s]
$P_J$	= distribution constant of species $J$ between organic and aqueous phases	[—]
$R_I$	= interfacial resistance	[s/cm]
$r_f$	= reaction rate for 1 : 2 complex formation	[mol/(cm <sup>3</sup> s)]
$t$	= time	[s]
$x$	= distance	[cm]
$x_L$	= length of stagnant layer	[cm]
$\beta$	= quantity defined by Eq. (15d)	[—]
$\Gamma_{HR}$	= interfacial excess quantity	[mol/cm <sup>2</sup> ]
$\Gamma_{HR}^o$	= saturated interfacial excess quantity	[mol/cm <sup>2</sup> ]
$\gamma$	= interfacial tension	[N/m]
$\gamma_a$	= quantity defined by Eq. (15e)	[—]
$\delta$	= thickness of interfacial zone	[cm]
$\varepsilon_J$	= molar extinction coefficient of species $J$	[cm <sup>2</sup> /mol]
$\tau$	= relaxation time	[s]

## <Subscripts>

$b$	= species in bulk of aqueous or organic phase
$CuR_2$	= 1 : 2 complex of copper and oxime
$e$	= value at equilibrium state
$f$	= forward extraction or forward reaction rate
$HR$	= <i>o</i> -hydroxyoxime
$i$	= species adjacent to interface
$R$	= dissociation species of <i>o</i> -hydroxyoxime
$r$	= stripping rate or reverse reaction rate



$t$  = value of total concentration

<Superscripts>

$b$  = value in bulk phase  
 $c$  = value for 1:2 complex  
 $d$  = value for dimer of hydroxyoxime  
 $m$  = value for monomer of hydroxyoxime  
 $*$  = value at interface  
 $-$  = species in organic phase

Literature Cited

- 1) Akiba, K. and H. Freiser: *Anal. Chim. Acta*, **136**, 329 (1982).
- 2) Carter, S. P. and H. Freiser: *Anal. Chim. Acta*, **136**, 511 (1980).
- 3) Debye, P.: *Trans. Electrochem. Soc.*, **82**, 265 (1942).
- 4) Flett, D. S., D. N. Okuhara and D. R. Spink: *J. Inorg. Nucl. Chem.*, **35**, 247 (1973).
- 5) Harada, M., M. Mori, M. Adachi and W. Eguchi: *J. Chem. Eng. Japan*, **16**, 184 (1983).
- 6) Harada, M., M. Mori, M. Adachi and W. Eguchi: *J. Chem. Eng. Japan*, **16**, 193 (1983).
- 7) Harada, M. and Y. Miyake: submitted to *J. Chem. Eng. Japan*.
- 8) Komasaawa, I., T. Otake and T. Muraoka: *J. Chem. Eng. Japan*, **13**, 204 (1980).
- 9) Komasaawa, I., T. Otake and A. Yamada: *J. Chem. Eng. Japan*, **13**, 209 (1980).
- 10) Matijevic, E.: "Surface and Colloid Science," Vol. 1, Wiley-Interscience (1969).
- 11) Miyake, Y., Y. Takenoshita and M. Teramoto: *J. Chem. Eng. Japan*, **16**, 203 (1983).
- 12) Miyake, Y., A. Mitsumoto and M. Teramoto: *Sol. Ext. and Ion Exchange*, **2** (7 & 8), 1069 (1984).
- 13) Miyake, Y., Y. Takenoshita and M. Teramoto: International Solvent Extraction Conference '83, p. 301 (1983).
- 14) Preston, J. S. and R. J. Whewell: *J. Inorg. Nucl. Chem.*, **39**, 1675 (1977).
- 15) Preston, S. J. and Z. B. Luklinska: *J. Inorg. Nucl. Chem.*, **42**, 431 (1980).
- 16) Preston, S. J.: *J. Inorg. Nucl. Chem.*, **42**, 441 (1980).
- 17) Tanaka, M. (ed.): Complex Reaction (Sakukeisei Hannou)," p. 318, Maruzen, Tokyo (1974).
- 18) Ueno, K. (ed.): "Chelate Chemistry," Nanko-do (1970).
- 19) Yoshizuka, K., K. Kondo and F. Nakashio: *J. Chem. Eng. Japan*, **18**, 163 (1985).

## HEAT TRANSFER IN HORIZONTAL PLUG AND SLUG FLOW FOR GAS-LIQUID AND GAS-SLURRY SYSTEMS

TOKIHIRO KAGO, TETSUYA SARUWATARI, MAKOTO KASHIMA,  
SHIGEHARU MOROOKA AND YASUO KATO

Department of Applied Chemistry, Kyushu University, Fukuoka 812

**Key Words:** Chemical Reactor, Heat Transfer, Preheater, Holdup, Pressure Drop, Three Phase Flow, Plug Flow, Slug Flow, Coal Liquefaction, Slurry

Heat transfer coefficients and flow characteristics were measured in a horizontal loop of 51.5 mm diam. pipe. The viscosities of liquid and slurry were changed in the range of 0.8–55 mPa·s. The experiments were carried out in the regimes of plug and slug flow.

The pressure drop in the straight sections was smaller than that predicted by the Lockhart-Martinelli correlation and was correlated by a newly proposed equation.

The gas holdup increased with increasing gas velocity and decreasing liquid or slurry velocity. A correlation of the gas holdup is presented.

The heat transfer coefficients,  $h$ , increased with increasing liquid velocity and decreased with increasing liquid viscosity. In the range of the superficial gas velocity  $U_g = 0.2\text{--}1\text{ m}\cdot\text{s}^{-1}$ ,  $h$  was nearly independent of the gas velocity. In the range of  $U_g = 1\text{--}10\text{ m}\cdot\text{s}^{-1}$ , however,  $h$  increased with increasing gas velocity. The values of  $h$  in the present experiments as well as those in the literature are well described by the equation proposed in this work.

### Introduction

Gas-liquid or gas-slurry flow is one of the most important features of chemical processes and is utilized for various purposes. In the direct coal liquefaction process, pulverized coal is mixed with a recycle solvent and is pumped into the preheater together

with hydrogen gas. During transportation in the preheater pipe, the gas and the slurry are heated up, and coal particles are virtually dissolved into the solvent. Thus, the performance of the preheater is strongly affected by its flow and heat transfer characteristics. In this paper, attention is confined to horizontal plug or slug flow, because the flow pattern is more complicated than that of other flow types and fewer works have been presented so far.

Received October 4, 1985. Correspondence concerning this article should be addressed to S. Morooka.